Convolutional Sparse Coding Network via Improved Proximal Gradient for Compressed Sensing Magnetic Resonance Imaging

Xiaofan Wang[1]
xy98067376@163.com
Yali Zhang[1]
hbzyl@stumail.ysu.edu.cn
Pengyu Li[1]
pyli80@163.com
Jinjia Wang[1,2]
wjj@ysu.edu.cn

[1] School of Information Science and Engineering
Yanshan University
Qinhuangdao, Hebei Province, China

[2] Hebei Key Laboratory of Information Transmission and Signal Processing,
Yanshan University
Qinhuangdao, Hebei Province, China

Abstract

Compressed sensing magnetic resonance imaging (CS-MRI) applies compressed sensing (CS) to effectively accelerate image reconstruction from undersampling k-space data. Compared with the traditional patch-based sparse representation of CS, the slice-based convolutional sparse coding (CSC) model makes up for the shortcomings of the sparse coding by establishing translation invariance. In this paper, based on the slice-based CSC model, we propose an improved proximal gradient algorithm to optimize image reconstruction performance. First, the variance regularization term is introduced into the CSC problem to remove the constraint on the convolutional dictionary. Second, we introduce the heavy ball system with dry friction from the dynamic system perspective to find a better local optimal solution. Then, the improved proximal gradient algorithm is unfolded into an encoder network to obtain the coding. The reconstruction process is modeled as a decoder network. The convolutional dictionary is updated by the backpropagation algorithm via the mean square error of the reconstructed signal. Compared with the current methods and the latest network, the proposed model-based novel network is demonstrated that it achieves better reconstruction performances.

1 Introduction

Magnetic resonance imaging (MRI) is a kind of tomography, that uses magnetic resonance to obtain electromagnetic signals from the human body and reconstruct human information. As one of the important medical diagnosis technologies, it can achieve high-resolution images, has high soft tissue contrast and no ionizing radiation to the human body, and provides a clear physiological and anatomical structure for the clinic. Due to its long time of data acquisition in k-space and slow imaging speed, some physiological motion artifacts [18] may be introduced in the imaging process, resulting in the decline of imaging quality and affecting the results of medical diagnosis. Therefore, reducing sampling time and ensuring accurate data reconstruction is of far reaching importance for clinical diagnosis.

In 2006, the theory of compressed sensing (CS) proposed by Candes [7] and Donoho [11] proved that as long as the finite equidistant condition (RIP) is satisfied, the original signal can be recovered under the condition that the sampling frequency is far lower than Nyquist. Due to the inherent compressibility of MRI data and the ability of MRI scanners to acquire frequency domain encoded samples, CSMRI can be used for effective sparse coding in wavelet, curving wave and other transform domains and then becomes the ideal solution for MRI reconstruction [19].

Sparse representation is one of the most popular prior mathematical modeling methods in various signal and image processing applications, widely used in image processing field [3], [10], [26]. In general, transformation that allows an image to have a sparse representation is called sparse transformation. Total variation (TV) [20] and wavelet transform [4] are two kinds of transforms commonly used in CS recovery problems. It is well known to use greedy algorithms (such as Orthogonal Matching Pursuit (OMP) [9]) or convex optimization algorithms to solve general sparse representation problems. In recent years, replacing image with patch and obtaining the local sparsity of sparse representation by learning transformation and learning dictionary (such as K-SVD [3] and MOD [12]) have gradually entered people's vision. This method of modeling signal data using the linear combination of several atoms in the learning dictionary, rather than predefined methods based on a global transform dictionary, has greatly improved the reconstruction quality of magnetic resonance images [14], [17]. Assuming that each image block has sparse representation, Ravishankar and Bresler [23] proposed a well-known two-step alternate method called Dictionary Learning-based MRI Reconstruction (DLMRI). This data-driven learning method greatly improved over previous methods based on predefined dictionaries.

However, this sparse representation method based on patch also has some defects [21]. When the sparse representation model is used to process images, it usually assumes that the trained image patches are independent of each other to obtain approximate global estimates. It ignores the correlation between image patches, resulting in a high degree of redundancy in the final result. Secondly, because its mathematical formula is essentially a linear combination of the learned surfaces, it cannot fully represent the image features of high frequency and high contrast, so some important details and texture parts of MR images are lost [15].

Zeiler *et al*. [29] proposed CSC, which uses convolution dictionary and convolution sum of convolution sparse coding coefficients to replace the linear combination of traditional methods. It generates different translation invariants and avoids overlapping face pieces to make up for the fundamental shortcomings of traditional sparse coding. CSC has been successfully applied to image reconstruction, image denoising and restoration [8], [16] in recent years. Papyan proposed a new convex relaxation algorithm through slice-based dictionary learning (SBDL) [21]. This algorithm adopts a local view, in which the sum of slices forms a signal block, which can train the convolution dictionary according to the local calculation in the signal domain to solve the global CSC problem. However, since the algorithm is based on the ADMM [6] solver in the signal domain, the convergence of the tracking algorithm, when the convolution dictionary is updated iteratively, is difficult to be proved. Peng [22] realized the joint and direct optimization of CDL problem under the non-convex and non-smooth optimization scheme and proposed a forward-backward splitting algorithm based on the Fourier domain. To solve the problem that the gradient descent algorithm can only ensure that the convergence result reaches the local lowest point rather than the global lowest point, Attouch [2] proposed IPGDF, a novel forward-backward splitting algorithm (convex). From the point of view of dynamic system, the algorithm discretizes the heavy ball system with friction (HBDF) by explicit implicit Euler, proving the algorithm's finite convergence.

In recent years, DNN has been introduced to CS to facilitate sampling and reconstruction due to its powerful learning ability. Some DNN-based algorithms have the advantages of adaptive solid learning ability and high reconstruction quality [25], [28]. Inspired by the Iterative Shrinkage Threshold algorithm and not strictly following the iterative optimization of ISTA, ISTA-Net [30] developed a general structured deep network to improve the ℓ_1-relaxation CS reconstruction. ADMM-Net [27] first proposed the deep architecture of CS-based MRI model derived from ADMM. Recently, a supervised convolutional sparse coding network (CSCNet) [24] based on ISTA algorithm and LISTA network has been used to solve the image denoising problem. It is trained by random gradient descent, but due to the use of ISTA iterative algorithm, it is easy to fall into local minima, resulting in poor results in the application of CSCNet in noise measurement.

This paper proposes a new CSC deep structure using an improved proximal gradient algorithm to realize CSMRI reconstruction. Firstly, due to the characteristics of sparse representation, we choose CSC to avoid some defects of sparse coding. To make the networking of the algorithm feasible, we introduce the variance regularization term into the optimization problem to eliminate the influence of local convolution dictionary on the network [13]. Secondly, because the general proximal gradient algorithm is difficult to find the global optimal solution quickly and accurately, we apply the inertial forward and reverse splitting algorithm ISTA-IDF from the dynamic system perspective to obtain better MRI reconstruction performance. By introducing DNN, we expand CSC into a deep network, improving the reconstruction efficiency. The reconstruction process is modeled as a decoder network, and the iterative process is carried out strictly according to the algorithm. Experiments show that our proposed MRI reconstruction framework has better reconstruction quality than the current deep network.

The rest of this paper is organized as follows. The second part introduces the improved CSC model using ISTA-IDF algorithm and the network architecture after CSC expansion. The third part gives the experimental results and demonstrates the performance comparison between the proposed method and other methods under different influencing factors. The fourth part summarizes the methods proposed in this paper and prospects the future work.

2 The Proposed Method

In this section, we describe in detail the process of reconstructing MR images through convolutional sparse coding. We first propose an ℓ_1 norm penalty optimization problem based on CSC to reconstruct MRI. The variables are updated by ISTA-IDF algorithm iteratively and finally expand the process into a deep network according to its iteration.

2.1 Convolutional Sparse Coding via Improved Proximal Gradient

Given a signal $\boldsymbol{X} \in \mathbb{R}^N$ and a matrix $\boldsymbol{D} \in \mathbb{R}^{N\times M}$ termed a convolutional dictionary, the sparse representation of $\boldsymbol{X}$ amounts to the solution for the following problem:

$$\arg\min_{\boldsymbol{\Gamma}} \frac{1}{2}\|\boldsymbol{X} - \boldsymbol{D}\boldsymbol{\Gamma}\|_2^2 + \lambda\Omega(\boldsymbol{\Gamma}) \,, \tag{1}$$

where the global signal $\boldsymbol{X}$ is a linear combination of a few columns, $\boldsymbol{\Gamma} \in \mathbb{R}^M$ is a sparse vector, Ω is the sparsity inducing function imposed on the sparse vector such as the ℓ_1 norm or the ℓ_0 norm, λ is the parameter that controls the sparsity level.

According to the slice-based approach for training the CSC model proposed by Papyan, the algorithm expresses the global signal as $\boldsymbol{X} = \sum_{i=1}^{N} \mathbf{P}_i^T \mathbf{D_L} \boldsymbol{\alpha}_i$. Where $\mathbf{D_L} \boldsymbol{\alpha}_i$ represents the i-th slice and $\mathbf{P}_i^T \in \mathbb{R}^N$ puts it in the i-th position and fills the rest with zeros. The sparse vector $\boldsymbol{\Gamma}$ is decomposed into a set of non-overlapping m-dimensional sparse vectors $\{\boldsymbol{\alpha}_i\}_{i=1}^N \in \mathbb{R}^m$ [21]. Considering the decomposition of $\boldsymbol{X}$ in terms of its slices and setting a ℓ_1 sparsity penalty as the regularization term, the above problem can be written as the following constrained minimization problem:

$$\underset{\boldsymbol{D}_L, \{\boldsymbol{\alpha}_i\}_{i=1}^N}{\arg\min} \ \frac{1}{2} \|\boldsymbol{X} - \sum_{i=1}^{N} \mathbf{P}_i^T \mathbf{D_L} \boldsymbol{\alpha}_i\|_2^2 + \lambda \sum_{i=1}^{N} \|\boldsymbol{\alpha}_i\|_1 \ . \tag{2}$$

This kind of minimization problem can be written in form $\underset{\mathbf{x}}{\arg\min} f(\mathbf{x}) + g(\mathbf{x})$, where f is a non-convex smooth function with Lipschitz continuous gradient, and g is a proper lower semicontinuous convex non-smooth function. To solve this type of problem, a dry friction damping $\partial\phi\left(\mathbf{x}'(t)\right)$ is introduced into the gravity ball system and the, HBDF system is shown below, where $\gamma > 0$ is a constant viscous damping parameter [2]:

$$\mathbf{x}''(t) + \gamma \mathbf{x}'(t) + \partial\phi\left(\mathbf{x}'(t)\right) + \bigtriangledown f\left(\mathbf{x}(t)\right) + \partial g\left(\mathbf{x}(t)\right) \ni 0 \ . \tag{3}$$

In this system, we use the characteristics of dry friction damping $\partial\phi\left(\mathbf{x}'(t)\right)$: the friction potential function ϕ is a lower semicontinuous convex function and has a sharp minimum at the origin. If the friction potential function ϕ satisfies the dry friction property (DF) with $B(0,r) \subset \partial\phi(0)$, we define that ϕ satisfies the property $(DF)_r$. According to the property of ϕ, we set $\phi(\mathbf{x}) = r_3\|\mathbf{x}\|_1$, where $r_3 > 0$ represents the dry friction threshold. Due to $\|\mathbf{x}\|_1$ having a sharp minimum value at the origin, from the perspective of dynamics when the resultant force of the system is less than the dry friction threshold, the speed becomes zero, and the system reaches a stable state.

Given $h > 0$ as the time step, we discretize the formula forward backward Euler and then obtain:

$$\begin{aligned} &\tfrac{1}{h^2}\left(\mathbf{x}^{k+1} - 2\mathbf{x}^k + \mathbf{x}^{k-1}\right) + \tfrac{\gamma}{h}\left(\mathbf{x}^{k+1} - \mathbf{x}^k\right) + \partial\phi\left(\tfrac{1}{h}\left(\mathbf{x}^{k+1} - \mathbf{x}^k\right)\right) \\ &\qquad + \bigtriangledown f\left(\mathbf{x}^k\right) + \partial g\left(\mathbf{x}^{k+1}\right) \ni 0 \end{aligned} \ . \tag{4}$$

ISTA-IDF introduces an auxiliary variable $\phi_k(\mathbf{x}) = h\phi\left(\frac{1}{h}\left(\mathbf{x} - \mathbf{x}_k\right)\right)$ to make $\partial\phi_k\left(\mathbf{x}^{k+1}\right) = \partial\phi\left(\frac{1}{h}\left(\mathbf{x}^{k+1} - \mathbf{x}^k\right)\right)$ hold, then we can get $\partial\phi_k + \partial g = \partial\left(\phi_k + g\right)$. Equation (4) could be simplified to:

$$\mathbf{x}^{k+1} + \frac{h^2}{1+\gamma h} \partial\left(\phi_k + g\right)\left(\mathbf{x}^{k+1}\right) \ni \mathbf{x}^k + \frac{1}{1+\gamma h}\left(\mathbf{x}^k - \mathbf{x}^{k-1}\right) - \frac{h^2}{1+\gamma h} \bigtriangledown f\left(\mathbf{x}^k\right) \ . \tag{5}$$

Finally we derive the iterative formula of ISTA-IDF algorithm from equation (5):

$$\mathbf{x}^{k+1} = \mathrm{prox}_{\lambda(\phi_k + \mathrm{g})}\left(\mathbf{x}^{k+1/2}\right) \ , \tag{6}$$

$$\mathbf{x}^{k+1/2} = \mathbf{x}^k + \beta\left(\mathbf{x}^k - \mathbf{x}^{k-1}\right) - \lambda \nabla \mathbf{f}\left(\mathbf{x}^k\right) \ , \tag{7}$$

where $\beta = \frac{1}{1+\gamma h}$ and $\lambda = \frac{h^2}{1+\gamma h}$.

2.2 MR Image Reconstruction with CSC

In order to solve the MRI reconstruction problem, we introduce ISTA-IDF proximal gradient descent algorithm into the general CSC model from the perspective of dynamics and add a variance regularization term to the formula to prevent a collapse in the ℓ_1 norm of the sparse vector [5], [13]. The improved optimization problem we finally get is as follows:

$$\underset{\{\boldsymbol{\alpha}_{l,i}\}}{\arg\min} \frac{1}{2}\sum_{l=1}^{I}\left\|\mathbf{F_u}\sum_{i=1}^{N}\mathbf{P}_i^T\mathbf{D_L}\boldsymbol{\alpha}_{l,i}-\boldsymbol{y}_l\right\|_2^2+r_1\sum_{l=1}^{I}\sum_{i=1}^{N}\left\|\boldsymbol{\alpha}_{l,i}\right\|_1+r_2\sum_{i=1}^{N}\left[\left(T-\sqrt{\mathrm{Var}\left(\boldsymbol{\alpha}_{\cdot i}\right)}\right)_+\right]^2, \tag{8}$$

where $\mathbf{D}_L$ is the local convolutional dictionary that has n rows and m columns; $\alpha_{l,i}$ is the sparse coding of each component i of each sample l; $\mathbf{P}_i^T$, which has N rows and n columns, is the operator that puts $\mathbf{D}_L\alpha_{l,i}$ in the i-th position and pads the rest of the entries with zero; r_1 and r_2 are both hyper-parameters. Considering the constraint function imposed on the sparse coefficient, we adopt the ℓ_1 norm constraint function. $\mathbf{F_u}\in\mathbb{R}^{M\times N}$ represents the partially sampled Fourier encoding matrix; $\boldsymbol{y}_l\in\mathbb{R}^M$ represents the partially sampled Fourier measurement and belongs to the group of image data $\boldsymbol{Y}=[\boldsymbol{y}_1,\boldsymbol{y}_2,...,\boldsymbol{y}_I]$. We apply $\boldsymbol{x}_l=\sum_{i=1}^{N}\mathbf{P}_i^T\mathbf{D_L}\alpha_{l,i}$ represents a set of reconstructed image data.

For this ℓ_1 non-smooth convex optimization model, we define f and g as follows:

$$f\left(\boldsymbol{\alpha}_{l,i}\right)=\frac{1}{2}\sum_{l=1}^{I}\left\|\mathbf{F_u}\sum_{i=1}^{N}\mathbf{P}_i^T\mathbf{D_L}\boldsymbol{\alpha}_{l,i}-\boldsymbol{y}_l\right\|_2^2+r_2\sum_{i=1}^{N}\left[\left(T-\sqrt{\mathrm{Var}\left(\boldsymbol{\alpha}_{\cdot i}\right)}\right)_+\right]^2, \tag{9}$$

$$g\left(\boldsymbol{\alpha}_{l,i}\right)=r_1\sum_{l=1}^{I}\sum_{i=1}^{N}\left\|\boldsymbol{\alpha}_{l,i}\right\|_1. \tag{10}$$

The first item of $f\left(\boldsymbol{\alpha}_{l,i}\right)$ is the data consistency item. The second item in equation (9) is over squared hinge terms involving the variance of each latent component $\alpha_{\cdot i}\in\mathbb{R}^n$ across the batch where $\mathrm{Var}\left(\boldsymbol{\alpha}_{\cdot i}\right)=\frac{1}{I-1}\sum_{l=1}^{I}\left(\boldsymbol{\alpha}_{l,i}-\boldsymbol{\mu}_i\right)^2$ and $\boldsymbol{\mu}_i$ is the mean across the i-th latent component, namely $\boldsymbol{\mu}_i=\frac{1}{I}\sum_{l=1}^{I}\boldsymbol{\alpha}_{l,i}$.

Then we apply ISTA-IDF algorithm to solve the optimization problem above. Introduce the intermediate variable $\left\{\alpha_{l,i}^{k+1/2}\right\}$, which is defined as

$$\boldsymbol{\alpha}_{l,i}^{k+1/2}=\boldsymbol{\alpha}_{l,i}^{k}+\beta\left(\boldsymbol{\alpha}_{l,i}^{k}-\boldsymbol{\alpha}_{l,i}^{k-1}\right)-\lambda\bigtriangledown f\left(\boldsymbol{\alpha}_{l,i}^{k}\right). \tag{11}$$

Consequently, the update rule of sequence $\left\{\boldsymbol{\alpha}_{l,i}^{k+1}\right\}$ we acquire is

$$\boldsymbol{\alpha}_{l,i}^{k+1}=\mathrm{prox}_{\lambda(\phi_k+g)}\left(\boldsymbol{\alpha}_{l,i}^{k+1/2}\right). \tag{12}$$

In order to get the sequence $\left\{\boldsymbol{\alpha}_{l,i}^{k+1}\right\}$, we need to calculate the gradient of the function f using the following formula:

$$\bigtriangledown_{\boldsymbol{\alpha}_{a,b}}f=\begin{cases}\mathbf{D_L^T}\mathbf{P}_a\mathbf{F}_u^T\left(\mathbf{F}_u\sum\limits_{i=1}^{N}\mathbf{P}_b^T\mathbf{D_L}\boldsymbol{\alpha}_{a,i}-\boldsymbol{y}_a\right)-\frac{2\beta}{I-1}\frac{T-\sqrt{\mathrm{Var}(\boldsymbol{\alpha}_{\cdot b})}}{\sqrt{\mathrm{Var}(\boldsymbol{\alpha}_{\cdot b})}}(\boldsymbol{\alpha}_{a,b}-\boldsymbol{\mu}_b) & \sqrt{\mathrm{Var}(\boldsymbol{\alpha}_{\cdot b})}<T\\ \mathbf{D_L^T}\mathbf{P}_a\mathbf{F}_u^T\left(\mathbf{F}_u\sum\limits_{i=1}^{N}\mathbf{P}_b^T\mathbf{D_L}\boldsymbol{\alpha}_{a,i}-\boldsymbol{y}_a\right) & otherwise\end{cases}. \tag{13}$$

Due to the function $\phi_k + g$ in the composite proximal mapping $\mathrm{prox}_{\lambda(\phi_k+g)}\left(\alpha_{l,i}^{k+1/2}\right)$ is the sum of two convex non-smooth functions (ℓ_1), the closed form solution of this proximal mapping can be obtained. For the variable $x \in \mathbb{R}$ and $a \in \mathbb{R}$ (current iteration value x_k of x), the proximal mapping can be modified to the following form:

$$\mathrm{prox}_{\lambda(\phi_k+g)}(x) = \arg\min_u \frac{1}{2}\|x-u\|_2^2 + \lambda r_1 \|u\|_1 + \lambda r_3 \|u-a\|_1 \ . \tag{14}$$

Decompose the above formula into a one-dimensional minimization problem of each component, for each $a \in \mathbb{R}$, set

$$T_a(x) = \arg\min_u \frac{1}{2}(x-u)^2 + \lambda r_1 |u|_1 + \lambda r_3 |u-a|_1 \ . \tag{15}$$

According to the definition of $T_a(x)$, it is easy to know that $T_a(x) = -T_{-a}(-x)$. The solution of $T_a(x)$ can be obtained only by calculating the solution at $a \geq 0$.

Using the differentiability of ℓ_1-regularization, the optimality condition can be got: $\lambda r_3 \partial|u-a|_1 + \lambda r_1 \partial|u|_1 \ni x-u$. Then the only closed form solution of $T_a(x)$ while $a \geq 0$ can be calculated in sections:

$$T_a(x) = \begin{cases} x - \lambda(r_1+r_3) & x > \lambda(r_1+r_3)+a \\ a & \lambda(r_1-r_3)+a < x \leq \lambda(r_1+r_3)+a \\ x-\lambda(r_1-r_3) & \lambda(r_1-r_3) < x \leq \lambda(r_1-r_3)+a \\ 0 & -\lambda(r_1+r_3) < x \leq \lambda(r_1-r_3) \\ x+\lambda(r_1+r_3) & x \leq -\lambda(r_1+r_3) \end{cases} . \tag{16}$$

In the end we obtain the solution of the proximal mapping $\mathrm{prox}_{\lambda(\phi_k+g)}(x)$ as:

$$\mathrm{prox}_{\lambda(\phi_k+g)}(x) = \begin{cases} T_a(x) & a \geq 0 \\ -T_{-a}(-x) & a \leq 0 \end{cases} . \tag{17}$$

The details of MRI reconstruction algorithm in ℓ_1-constrained CSC model are described in Algorithm 1.

Algorithm 1 ℓ_1-constrained convolutional sparse coding in MR image reconstruction.

Input: Partially sampled Fourier measurement $\boldsymbol{y}_l$, local convolutional dictionary $\mathbf{D_L}$

Output: Estimated coding $\boldsymbol{\alpha}_{l,i}^k$.

Initialization: $\boldsymbol{\alpha}_{l,i}^0 = \boldsymbol{\alpha}_{l,i}^1, \gamma > 0, h < \frac{2\gamma}{L}$

For iteration $k = 0 : K-1$

compute $\triangledown f\left(\boldsymbol{\alpha}_{l,i}^k\right)$ using equation (13)

$\boldsymbol{\alpha}_{l,i}^{k+1/2} = \boldsymbol{\alpha}_{l,i}^k + \frac{1}{1+\gamma h}\left(\boldsymbol{\alpha}_{l,i}^k - \boldsymbol{\alpha}_{l,i}^{k-1}\right) - \frac{h^2}{1+\gamma h} \triangledown f\left(\boldsymbol{\alpha}_{l,i}^k\right)$,

$\boldsymbol{\alpha}_{l,i}^{k+1} = \mathrm{prox}_{\frac{h^2}{1+\gamma h}(\phi_k+g)}\left(\boldsymbol{\alpha}_{l,i}^{k+1/2}\right)$,

end for

2.3 Iterative Neural Network via Unfolding CSC

We expand the proposed method to improve MRI reconstruction into a structured network. The network structure is composed of a series of blocks, each corresponding to an iteration of the proposed reconstruction method. In practice, we use DNNs composed of convolutional and deconvolutional layers to realize the iteration of variables, as shown in Figure 1. Matrix multiplication $\mathbf{D_L}\boldsymbol{\alpha}_{l,i}$ can be replaced by convolution operation $\boldsymbol{d}_m * \boldsymbol{\alpha}_{l,i}$. $\{\boldsymbol{d}_m\}$ and $\{\boldsymbol{\alpha}_{l,i}\}$ can be naturally viewed as the convolutional kernels and feature maps in DNNs, respectively, where m is the filter number. The partially sampled Fourier encoding matrix $\mathbf{F_u}$ is fixed.

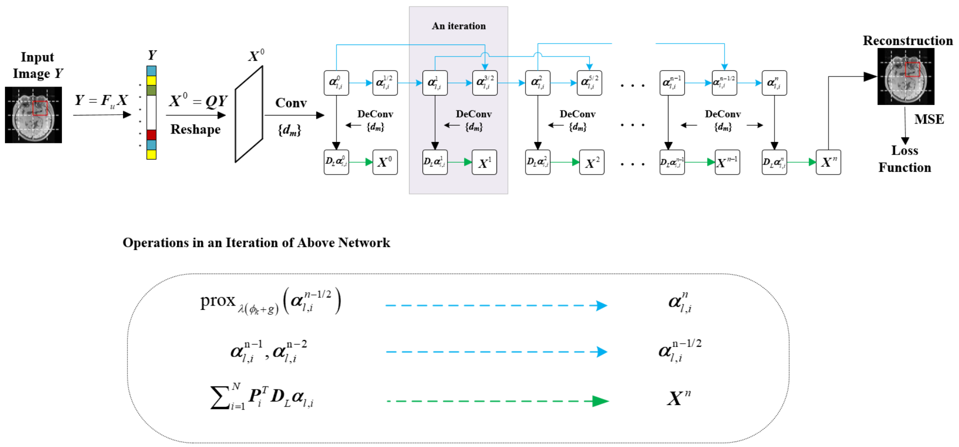

Figure 1: The framework of the proposed iterative neural network design via unfolding CSC.

In the end, we apply the mean square error (MSE) between the original image $\boldsymbol{Y}$ and the reconstructed $\boldsymbol{X}^n$ to represent the total loss function:

$$L_{MSE} = \|\boldsymbol{Y} - \boldsymbol{X}^n\|_2^2. \tag{18}$$

Where $\boldsymbol{X}^n$ is the reconstruction result of the n-th iteration. Considering the termination criterion, it requires the residual $\boldsymbol{s}^{k+1} = \boldsymbol{\alpha}_{l,i}^{k+1} - \boldsymbol{\alpha}_{l,i}^{k}$ must be small according to [6].

3 Experimental Results

Several groups of comparative experiments are set up to compare the performance of the proposed method with others, such as ISTA-Net+, ADMM-Net and l_0-CSC-Net [25]. For fairness, we train these methods on the same randomly selected 50 images. The size of images we use in the synthetic experiments is 512×512, and data acquisition is simulated by subsampling the two-dimensional discrete Fourier transform of the MR images. The measurement matrix $F_u \in \mathbb{R}^{M \times N}$ is generated as a random Gaussian matrix. In the test phase, the trained network adopts Peak Signal-to-Noise Ratio (PSNR) as the evaluation standard. In order to further verify the stability of the proposed method, we also conduct reconstruction experiments on the polluted images, and compare it with the advanced IDPCNN method [1]. All of the above experiments were implemented on a PC configured with Intel (R) Core (TM) I5-8265U CPU @ 1.60ghz and 4G Byte RAM.

3.1 Reconstruction performance under different undersampling ratios

In this part, we evaluate the reconstruction performance of the proposed method under different undersampling ratios. Our method is compared with the advanced ISTA-Net+, ADMM-Net and l_0-CSC-Net algorithms, and PSNR(dB) is used for evaluation. We adopt pseudo radial as the sampling scheme and five undersampling ratios (10%, 20%, 30%, 40% and 50%) during the experiment to obtain the Fourier measurements. The corresponding PSNRs are given in Table 1.

Methods	Undersampling ratios				
	10%	20%	30%	40%	50%
Proposed	**38.46**	**39.75**	**41.32**	42.47	43.79
ADMM-Net	26.98	29.74	31.82	34.23	35.32
l_0-CSC-Net	27.70	31.92	34.09	35.55	36.89
ISTA-Net+	37.16	38.73	40.89	**42.52**	**44.09**

Table 1: Reconstruction performance in PSNR (dB) under different undersampling ratios.

As shown in Table 1, our method generally performs better than other methods under lower MRs, which may be because, for higher levels of sparsity, using variance regularization on the codes can better utilize the multi-layer structure of the convolution network [13]. When the under-sampling ratio is 40%, its reconstruction performance is nearly equal to that of the advanced ISTA-Net+ algorithm. We further compare the time required for the reconstruction by these methods. The reconstruction time data per epoch in Table 2 shows that our method can complete the reconstruction at a quite fast speed.

Methods	Proposed	ADMM-Net	l_0-CSC-Net	ISTA-Net+
Times(seconds)	0.0618	0.8026	0.0698	0.1467

Table 2: Average reconstruction time of different methods.

3.2 Experiments on Noisy Data

In order to test the sensitivity of the proposed method to images polluted by complex Gaussian white noise, we tested the reconstruction quality. We choose the human brain test diagram Figure 2 (a) for the noise experiment. A complex valued Gaussian white noise with standard deviation σ= 0.03 is added to the k-space data sampled from Figure 2 (a) under 30% pseudo radial sampling pattern, to obtain the polluted image Figure 2 (b). Then we test the reconstruction quality and error performance of ISTA-Net+, ADMM-Net, l_0-CSC-Net, IDPCNN and our method. The reconstruction results are shown in Figs 2 (c)-(g). The corresponding error magnitudes of the reconstruction are displayed in Figs 2 (h)-(l).

Although the reconstructed images of ISTA-Net+ and IDPCNN are relatively clear, the residual image effects are average. l_0-CSC-Net performs good in the residual image effects, but the textures and edges of the reconstructed image are not clear enough. The reconstructed image performs well in image contour and detail texture restoration. It can indicate that our method provides a more accurate reconstruction of image contrast and richer details in noisy cases.

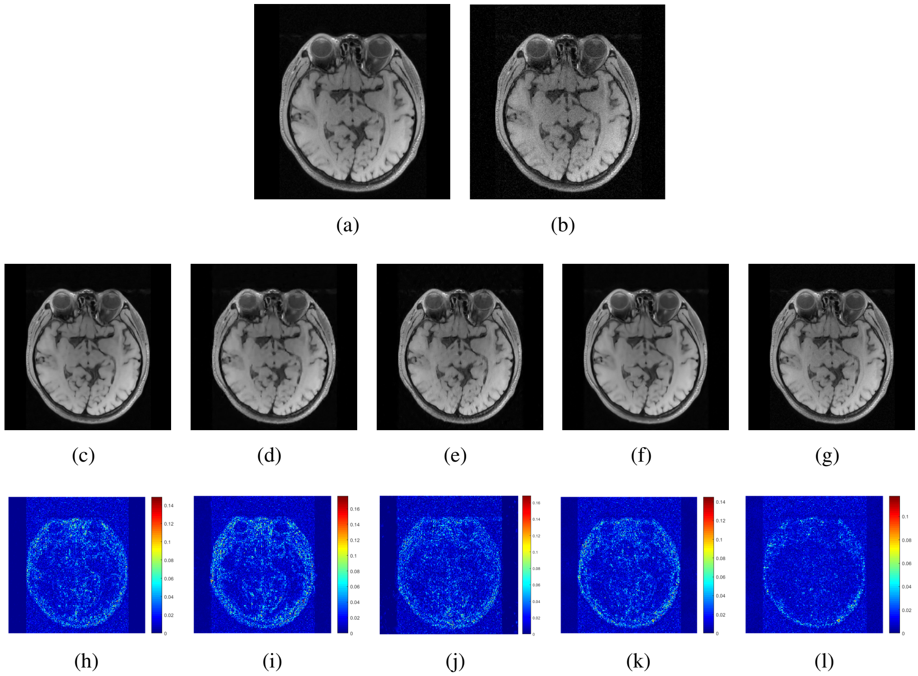

Figure 2: Reconstruction results of the image under different noise levels. From left to right are of ISTA-Net+, ADMM-Net, l_0-CSC-Net, IDPCNN and our method.

4 Conclusion

In this paper, we propose a model-based structured deep network to realize MRI reconstruction. The proposed network makes use of the advantages of CSC and deep learning at the same time. Based on the CSC model, the improved ISTA-IDF algorithm is introduced and expanded into a network with better convergence speed in the MRI reconstruction process. Experimental results show that the proposed network performs better at a low sampling rate and ensures that the reconstructed image is clearer and has more detailed information while speeding up the reconstruction process than the state-of-the-art methods.

Acknowledgements

We thank referee for comments that greatly improved the manuscript. Thanks to Jin Li and Ze Li of Yanshan University for their help in programming and experiment. This work was supported in part by Basic Research Cooperation Projects of Beijing, Tianjin and Hebei (19JCZDJC65600(Z), F2019203583), and the Central Funds Guiding the Local Science and Technology Development (Basic Research Projects)(206Z5001G).

References

[1] Idpcnn: Iterative denoising and projecting cnn for mri reconstruction. *Journal of Computational and Applied Mathematics*, 2022. https://www.sciencedirect.com/science/article/pii/S0377042721005719, author = Ruizhi Hou and Fang Li,.

[2] Samir Adly and Hedy Attouch. First-order inertial algorithms involving dry friction damping. *Mathematical Programming*, 193(1):405–445, 2022.

[3] M. Aharon, M. Elad, and A. Bruckstein. K-svd: An algorithm for designing overcomplete dictionaries for sparse representation. *IEEE Transactions on Signal Processing*, 54(11):4311–4322, 2006.

[4] Mehmet Akçakaya, Seunghoon Nam, Peng Hu, Mehdi H. Moghari, Long H. Ngo, Vahid Tarokh, Warren J. Manning, and Reza Nezafat. Compressed sensing with wavelet domain dependencies for coronary mri: A retrospective study. *IEEE Transactions on Medical Imaging*, 30(5):1090–1099, 2011.

[5] Adrien Bardes, Jean Ponce, and Yann LeCun. VICReg: Variance-invariance-covariance regularization for self-supervised learning. In *International Conference on Learning Representations*, May 2022. https://openreview.net/forum?id=xm6YD62D1Ub.

[6] S. Boyd, N. Parikh, E. Chu, B. Peleato, and J. Eckstein. Distributed optimization and statistical learning via the alternating direction method of multipliers. *Foundations & Trends in Machine Learning*, 3(1):1–122, 2010.

[7] E.J. Candes, J. Romberg, and T. Tao. Robust uncertainty principles: exact signal reconstruction from highly incomplete frequency information. *IEEE Transactions on Information Theory*, 52 (2):489–509, 2006.

[8] Boheng Chen, Jie Li, Biyun Ma, and Gang Wei. Convolutional sparse coding classification model for image classification. In *2016 IEEE International Conference on Image Processing (ICIP)*, pages 1918–1922, 2016.

[9] S. CHEN, S. A. BILLINGS, and W. LUO. Orthogonal least squares methods and their application to non-linear system identification. *International Journal of Control*, 50(5):1873–1896, 1 1989.

[10] Weisheng Dong, Lei Zhang, Guangming Shi, and Xiaolin Wu. Image deblurring and super-resolution by adaptive sparse domain selection and adaptive regularization. *IEEE Transactions on Image Processing*, 20(7):1838–1857, 2011.

[11] D.L. Donoho. Compressed sensing. *IEEE Transactions on Information Theory*, 52(4):1289–1306, 2006.

[12] K. Engan, S.O. Aase, and J. Hakon Husoy. Method of optimal directions for frame design. In *1999 IEEE International Conference on Acoustics, Speech, and Signal Processing. Proceedings. (ICASSP99)*, pages 2443–2446, 1999.

[13] Katrina Evtimova and Yann LeCun. Sparse coding with multi-layer decoders using variance regularization. *Transactions on Machine Learning Research*, 2022. https://openreview.net/forum?id=4GuIi1jJ74.

[14] Yue Huang, John Paisley, Qin Lin, Xinghao Ding, Xueyang Fu, and Xiao-Ping Zhang. Bayesian nonparametric dictionary learning for compressed sensing mri. *IEEE Transactions on Image Processing*, 23(12):5007–5019, 2014.

[15] Xiong Jiaojiao, Lu Hongyang, Zhang Minghui, and Liu Qiegen. Convolutional sparse coding in gradient domain for mri reconstruction. *Acta Automatica Sinica*, 43(10):1841–1849, 2017.

[16] Alex Krizhevsky, Ilya Sutskever, and Geoffrey E. Hinton. Imagenet classification with deep convolutional neural networks. *Communications of the ACM*, 60(6):84–90, 1 2017.

[17] Jiansen Li, Ying Song, and Jun Zhao. Dual-dictionary learning based mr image reconstruction with self-adaptive dictionaries. In *2015 37th Annual International Conference of the IEEE Engineering in Medicine and Biology Society (EMBC)*, pages 7051–7054, 2015.

[18] Michael Lustig, David Donoho, and John M Pauly. Sparse mri: The application of compressed sensing for rapid mr imaging. *Magnetic Resonance in Medicine*, 58(6):1182–1195, 2007.

[19] Michael Lustig, David L. Donoho, Juan M. Santos, and John M. Pauly. Compressed sensing mri. *IEEE Signal Processing Magazine*, 25(2):72–82, 2008.

[20] Lustig M, Donoho D, and Pauly JM. Sparse mri: The application of compressed sensing for rapid mr imaging. *Magnetic resonance in medicine: official journal of the Society of Magnetic Resonance in Medicine*, 58(6):1182–1195, 1 2007.

[21] Vardan Papyan, Yaniv Romano, Michael Elad, and Jeremias Sulam. Convolutional dictionary learning via local processing. In *2017 IEEE International Conference on Computer Vision (ICCV)*, pages 5306–5314, 2017.

[22] Guan-Ju Peng. Joint and direct optimization for dictionary learning in convolutional sparse representation. *IEEE Transactions on Neural Networks and Learning Systems*, 31(2):559–573, 2020.

[23] Saiprasad Ravishankar and Yoram Bresler. Mr image reconstruction from highly undersampled k-space data by dictionary learning. *IEEE Transactions on Medical Imaging*, 30(5):1028–1041, 2011.

[24] Dror Simon and Michael Elad. Rethinking the csc model for natural images. In *2019 Neural Information Processing Systems (NeurIPS)*, pages 2274–2284, 2019.

[25] Jiaqi Sun, Wenrui Dai, Chenglin Li, Junni Zou, and Hongkai Xiong. Compressive sensing via unfolded ℓ_0 -constrained convolutional sparse coding. In *2021 Data Compression Conference (DCC)*, pages 183–192, 2021.

[26] John Wright, Allen Y. Yang, Arvind Ganesh, S. Shankar Sastry, and Yi Ma. Robust face recognition via sparse representation. *IEEE Transactions on Pattern Analysis and Machine Intelligence*, 31(2):210–227, 2009.

[27] Yan Yang, Jian Sun, Huibin Li, and Zongben Xu. Deep admm-net for compressive sensing mri. In *Proceedings of the 30th International Conference on Neural Information Processing Systems*, pages 10–18, 2016.

[28] Hantao Yao, Feng Dai, Shiliang Zhang, Yongdong Zhang, Qi Tian, and Changsheng Xu. Dr2-net: Deep residual reconstruction network for image compressive sensing. *Neurocomputing*, pages 483–493, 2019.

[29] Matthew D. Zeiler, Dilip Krishnan, Graham W. Taylor, and Rob Fergus. Deconvolutional networks. In *2010 IEEE Conference on Computer Vision and Pattern Recognition (CVPR)*, pages 2528–2535, 2010.

[30] Jian Zhang and Bernard Ghanem. Ista-net: Interpretable optimization-inspired deep network for image compressive sensing. In *2018 IEEE/CVF Conference on Computer Vision and Pattern Recognition*, pages 1828–1837, 2018.